Lateral Turbulence Intensity and Plume Meandering During Stable Conditions

STEVEN R. HANNA

Environmental Research & Technology, Inc., Concord, MA 01719

(Manuscript received 27 December 1982, in final form 19 March 1983)

ABSTRACT

There is much evidence in the literature for the presence of mesoscale lateral meanders in the stable nighttime boundary layer. These meanders result in relatively high lateral turbulence intensities and diffusion rates when averaged over an hour. Anemometer data from 17 overnight experiments at Cinder Cone Butte in Idaho are analyzed to show that the dominant period of the mesoscale meanders is about two hours. Lidar cross-sections of tracer plumes from these same experiments show that the hourly average σ_y is often dominated by meandering. Since meandering is not always observed for given meteorological conditions, it is suggested that nighttime diffusion cannot be accurately predicted without using onsite observations of wind fluctuations. In case no turbulence data are available, an empirical formula is suggested that predicts the hourly average lateral turbulence intensity as a function of wind speed and hour-to-hour variation in wind direction.

1. Introduction

Similarity theory is adequate for estimating turbulence and diffusion during unstable and neutral conditions in the planetary boundary layer. It is also satisfactory for the vertical component of turbulence during stable conditions, since vertical turbulence levels approach zero as stability increases. In these conditions, turbulent energy components σ_v^2 and σ_w^2 are functions of u_* or w_*, z/L, and z_i/L. The parameters σ_v and σ_w are the standard deviations of the lateral and vertical components of turbulent velocity, u_* the friction velocity, L the Monin–Obukhov length, z_i is mixing depth, z is elevation, and w_* the convective scaling velocity $[w_* = (gQ_0z_i/T)^{1/3}]$. The parameter Q_0 is the surface heat flux. Similarity theory does not apply to the lateral component σ_v^2 during stable conditions, when mesoscale eddies or lateral meandering may possibly dominate the measured value (Pasquill, 1974). Several examples of observations of meandering are reviewed in Section 2, providing background for these conclusions and illustrating how the lateral turbulence intensity σ_v/u is a function of wind speed and hour-to-hour variations in wind direction during light-wind stable conditions. This functional dependence is not accounted for by EPA regulatory models but is suggested in some NRC regulatory models (Nuclear Regulatory Commission Regulatory Guide 1.145).

In Section 3 evidence is given of increased lateral turbulence and diffusion due to mesoscale eddies with period 1 to 4 hours at Cinder Cone Butte, Idaho. The first field experiment of EPA's Complex Terrain Model Development (CTMD) program took place in 1980 at Cinder Cone Butte (CCB) (Lavery *et al.*, 1982). This is a multi-year program with the purpose of development of diffusion models for regulatory application in complex terrain. The CCB is an isolated 100 m symmetrical hill located on a flat plain in the Snake River Basin. The field study included ten flow visualization (oil–fog) experiments and 18 multi-hour tracer gas experiments conducted during stable flow conditions. Supporting meteorological, photographic and lidar data were acquired. Because the principal 150 m meteorological tower was sited in a location outside the zone perturbed by CCB during easterly and west-northwesterly stable winds and because the oil–fog and tracer gas release location (via a mobile crane) was typically 1 km upwind of CCB, the tower and source data do not reflect the butte's perturbation and can be analyzed as if they were taken over flat terrain. Considerable lateral meandering of the plume was often observed during light-wind stable conditions. In this study, time series analysis techniques are used to estimate the time scales of these mesoscale fluctuations. Energy spectra and autocorrelograms are used as a basis for estimation of time scales. Lidar cross-sections of the plume upwind of the butte also illustrate the meandering of the plume centroid and its influence on hourly averaged plume spread. Finally, the 136 hours of data are used to verify an empirical formula that permits the hourly average lateral turbulence intensity to be estimated from hourly average wind speed and direction records.

2. Background

Current models of atmospheric diffusion at short distances in the boundary layer are generally satisfactory for nearly-neutral stabilities. The parameters of the Gaussian plume model, which is used for most regulatory applications, are best defined for those conditions. Furthermore, other diffusion models, such as similarity theory and K theory models, are most dependable in the neutral limit, where the Monin–Obukhov length L does not enter the problem. Studies of the unstable boundary layer (Deardorff, 1974) suggest that diffusion under unstable conditions is determined by the convective velocity scale w_* and the mixing depth z_i. However, on the stable side, boundary layer parameters and diffusion are well-determined only for slightly stable conditions when there is sufficient mechanical turbulence generated to assure that the atmosphere is well-mixed (critical Richardson number less than about one). Vertical turbulence and diffusion rates are small, and as a consequence of the three-dimensional nature of small scale turbulence, diffusion due to small scale eddies in all three components is reduced. However, two-dimensional mesoscale horizontal eddies are not suppressed by vertical stability forces and are produced by gravity waves, terrain interactions with the flow, mesoscale rolls and cell patterns in the synoptic flow or surface inhomogeneities. Their effect on plumes is usually recognized as a slow meandering of the plume; i.e., the instantaneous plume may be thin but over a time period of an hour or more it may meander over a wide angle.

Pasquill (1974) briefly reviews the variation of the standard deviation of wind direction fluctuations σ_θ during stable conditions, where σ_θ is related to the lateral turbulence intensity $i_y = \sigma_v/u$, by the formula,

$$\tan\sigma_\theta = \sigma_v/u = i_y. \qquad (1)$$

This parameter is important for calculating diffusion because it is used in the following relation for σ_y (Pasquill, 1976):

$$\sigma_y = i_y x F_y(x),$$
$$(i_y = \sigma_\theta \quad \text{for small } \sigma_\theta) \qquad (2)$$

where σ_y is the standard deviation of the lateral concentration distribution in the plume, and $F_y(x)$ a dimensionless function that is close to unity at distances less than 1 km from the source and drops to about 0.5 to 0.8 at a distance of 10 km. Pasquill presents data observed by Smith and Abbott (1961), which are reproduced here as Fig. 1, illustrating that σ_θ increases as winds become light at night (i.e., as stability increases). The best fit line through these data suggest that at that particular measurement site (Porton, England) during stable conditions, σ_v is relatively insensitive to both wind speed and stability (in fact σ_v retains a value of about 0.3 m s^{-1} for all wind speeds during stable conditions).

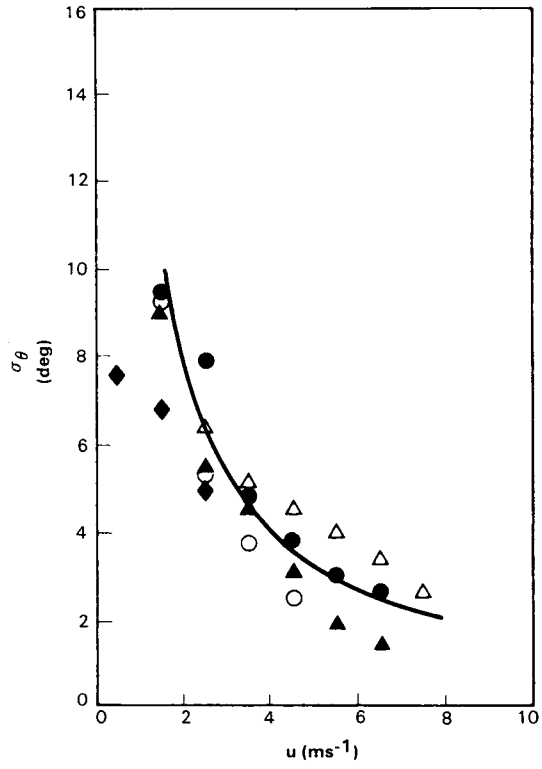

FIG. 1. Wind direction fluctuation as a function of wind speed and stability observations (from Smith and Abbott 1961) at a height of 16 m over open grassland, Porton.

Similar results were obtained from a complex terrain site in California by Hanna (1981a) during nighttime conditions, who found that a constant value of σ_v ($\approx\sigma_\theta u$) of about 1 m s^{-1} is most appropriate for this site, independent of wind speed. It seems reasonable that the larger value of σ_v in California is due to lateral eddies induced by the terrain (measurement heights were not much different—16 m in England and 10 m in California). The analysis further illustrated the large variability in σ_θ at low wind speeds for σ_θ was found to vary between 20 and 100° at a wind speed of 1 m s^{-1}.

An another example Schacher *et al.* (1982) found that σ_θ was relatively large and variable during stable conditions for an overwater diffusion experiment performed off the California coast. A constant value of

σ_v of about 0.5 m s^{-1} is appropriate for these data. They attributed their observations of large σ_θ to local mesoscale eddies caused by sea breeze interactions with the coastal mountains or flow around the channel islands, but Lemone (1978) states that "the importance of the mesoscale over the ocean emphasizes the tendency of the atmosphere to introduce these scales even without forcing from an irregular lower boundary." Mesoscale eddies or meandering can occur anywhere in the earth's planetary boundary layer, no matter how flat and uniform the surface.

Standard Environmental Protection Agency regulatory guidance (e.g., as summarized by Gifford 1976) still supports the use of Pasquill–Gifford stability classes determined from winds, cloud cover, and radiation. The Nuclear Regulatory Commission sometimes permits the determination of stability class from σ_θ by means of the following monotonic relationship between Pasquill stability class and σ_θ:

Pasquill class	A	B	C	D	E	F
σ_θ (deg)	≥22.5	17.5–22.5	12.5–17.5	7.5–12.5	3.8–7.5	<3.8

This is a conservative approach, for we see from the data reported by Pasquill (1974), Hanna (1981a) and Schacher *et al.* (1982) that σ_θ is only occasionally observed to be small during stable condition (classes E or F), and usually σ_θ is much larger. The EPA and NRC do allow in special circumstances the use of observed values of σ_θ to estimate σ_y from a method such as that in Eq. (1), but special permission is required for each application. The Nuclear Regulatory Commission (NRC, 1979) has recognized this inconsistency between the Pasquill class and the σ_θ's given in the above table, and has sponsored a series of tracer experiments during light-wind, stable conditions (e.g., Sagendorf and Dickson, 1974; VanderHoven, 1976). Sagendorf and Dickson report observations of hourly average σ_θ from 12 to 72° for wind speeds ranging from 0.8 to 1.9 m s^{-1}. The information in these experiments as well as several other field experiments was condensed into a set of tentative empirical correction factors for σ_y for lateral meander suggested in NRC Regulatory Guide 1.145 (see Figure 2). According to these procedures σ_y would be calculated using standard Pasquill–Gifford–Turner techniques and then multiplied by the factor M which is as high as 6.0 for stability class G and wind speeds less than 2 m s^{-1}. The NRC stresses that this guidance is preliminary and needs testing.

Kristensen *et al.* (1981) developed a mathematical model for stable diffusion based on Taylor's statistical theory, where it is required that the time scale of the meandering eddies be known. They used meteorological data from Riso, Denmark, and the small island of Sprogo to show that, as a rule, meandering is present in a strongly stable atmosphere with low wind speeds. Values of σ_y for an averaging time of three hours at a downwind distance of 20 km were calculated from their theory using Riso data with the result that σ_y is seen to be largest for strongly stable conditions with light wind speeds. The "best fit" line from their calculations is given by the formula,

$$\sigma_y = 5400u^{-0.8},$$

(σ_y in m at x = 20 km, u in m s^{-1}). (3)

All the evidence in the report by Kristensen *et al.* and the other papers reviewed above suggests that i_y, σ_θ, and σ_y are often large during light-wind, stable conditions. In the remainder of this paper, we provide further evidence for this effect from a diffusion experiment at Cinder Cone Butte, Idaho, analyze the spectral characteristics of the lateral mesoscale eddies or meanders that produce this effect, and suggest a simple empirical formula for stable i_y.

3. Time series analysis of wind speed data at Cinder Cone Butte

The purpose of the EPA-sponsored field study at Cinder Cone Butte was to aid in the development of a diffusion model for plume impaction on elevated terrain. Experiments took place on several nights during October 1980, and tracer releases were from ele-

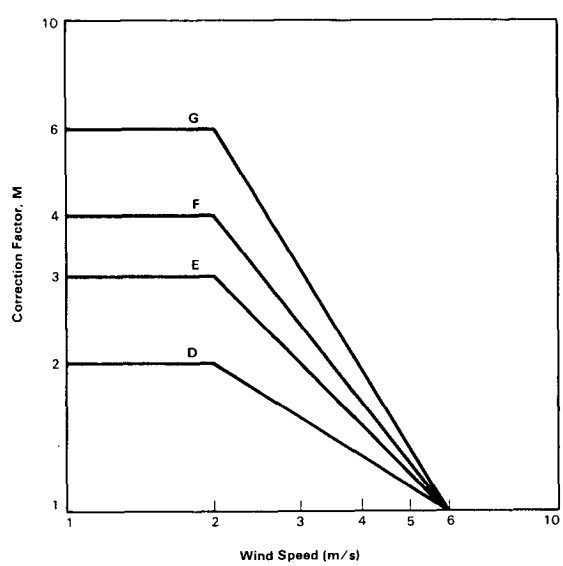

FIG. 2. Correction factors for Pasquill-Gifford σ_y values due to meander, based on a figure in NRC Regulatory Guide 1.145. The letters G, F, E, D denote the stability class based on $\Delta T/\Delta z$.

vations varying from ~20 to ~80 m. Wind speed data were obtained from three-component propeller anemometers at the 40 or 80 m levels on a 150 m tower. Since the butte is a relatively small hill on an otherwise flat plain, the measurements upwind of the butte can be treated as if they are representative of flow over a flat surface. These wind observations confirm the findings at other sites reported in Section 2. The 8 h wind records are characterized by slow fluctuations in wind speed and direction. Meanders or mesoscale fluctuations are evident on strip charts of wind velocity and suggest time periods on the order of 10 min to several hours. Some of the CCB experiments exhibit exceptional variability in wind speed and direction. For example, a time series of the 5 min average u-component wind speed from the 40 m level of the 150 m tower for Experiment 207 from 0000 to 0800 LST 25 October 1980 is plotted in Fig. 3. Eddies with periods of 30 min to 2 h are apparent on this figure. In a few of the 8 h experiments at CCB the wind direction went completely around the compass during the period.

Energy spectra of the wind speed during stable nighttime conditions were calculated for seventeen CCB experiments of eight-hour duration. A standard Fast Fourier Transform (FFT) computer code was applied to the u and v components of the wind speed for each experiment. A linear trend was removed from each time series, since a trend will show up in the spectrum as a great deal of energy at the lowest frequency point. Also the beginning and end of the time series were smoothed to prevent unrealistic behavior of the spectrum at high frequencies (Rayment, 1970; Cooley and Tukey, 1965). Autocorrelograms and spectra were plotted for each experiment. The autocorrelogram and energy spectrum for the data in Fig. 3 are given in Figs. 4 and 5. The autocorrelogram indicates strong cyclic behavior, reaching a minimum of −0.65 at a time lag of 50 min and a secondary maximum of 0.40 at a time lag of about 120 min. The spectrum is seen to contain the most energy in the frequency range from about 0.2 to 1 cycles per hour.

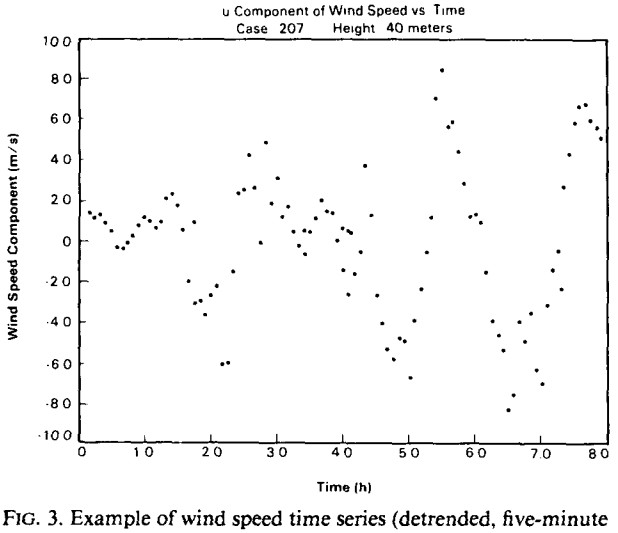

FIG. 3. Example of wind speed time series (detrended, five-minute averages) for Run 207 (0000 to 0800 LST 25 October 1980).

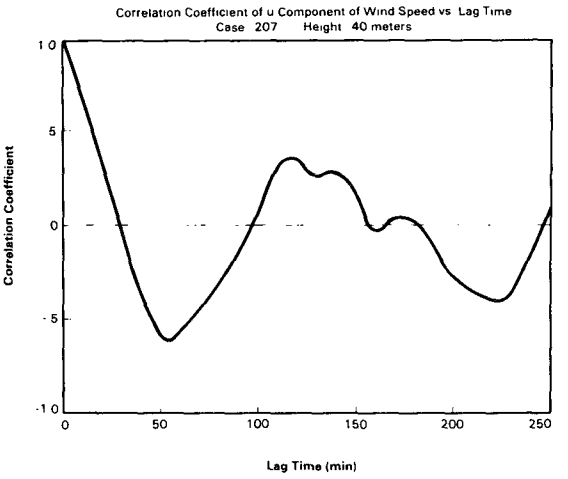

FIG. 4. Autocorrelogram for data in Fig. 3.

A summary of the time series analysis of 17 of the CCB experiments is given in Table 1. Wind observations at the 40 m level of the 150 m tower were used if available; otherwise, the winds at the 80 m level were used. The time period T_{max} at which maximum turbulent energy occurs is estimated by two procedures:

- Autocorrelogram method: $T_{max} = 5T(e^{-1})$, where $T(e^{-1})$ is the time lag when the autocorrelogram first drops to e^{-1} or 0.37. The time period T_{max} of the turbulent fluctuation associated with $T(e^{-1})$ is obtained by multiplying by 5. The factor 5 comes from cal-

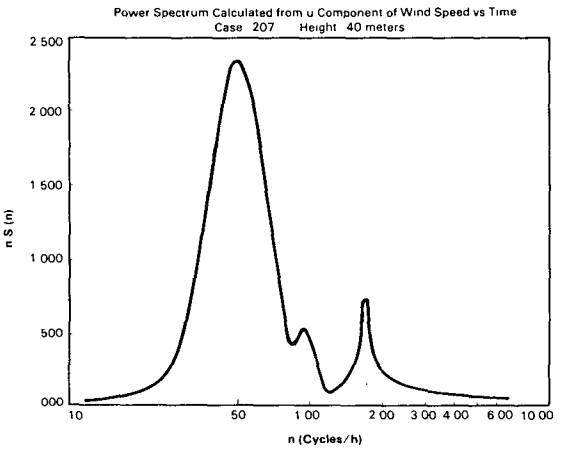

FIG. 5. Power spectrum for data in Fig. 3.

TABLE 1. Time scales as estimated by the spectral and autocorrelogram techniques for 34 CCB time series.

Run	Wind component	Height (m)	Time scale (min) from spectrum	Time scale (min) from autocorrelogram
201	u	40	100	80
201	v	40	120	110
202	u	40	86	85
202	v	40	120	140
203	u	40	50	100
203	v	40	120	125
204	u	40	67	100
204	v	40	55	100
205	u	80	200	175
205	v	80	120	115
206	u	80	120	85
206	v	80	150	160
207	u	40	100	85
207	v	40	150	125
208	u	40	120	135
208	v	40	120	135
209	u	40	120	85
209	v	40	55	50
210	u	80	200	175
210	v	80	100	50
211	u	80	100	110
211	v	80	120	150
213	u	40	120	140
213	v	40	240	200
214	u	40	240	275
214	v	40	120	100
215	u	40	210	110
215	v	40	240	250
216	u	40	—	250
216	v	40	240	200
217	u	40	240	100
217	v	40	86	125
218	u	40	240	150
218	v	40	240	175
	Median		120 min	125 min
	Range		50–240 min	50–275 min

culating the spectrum for a sinusoidal fluctuation (Hanna, 1981b).

- Spectral method: T_{max} is the period associated with maximum $nS(n)$, where n is frequency and S is energy density in units of $m^2\ s^{-2}$ per unit frequency.

The T_{max} values determined by the autocorrelogram and spectral methods agree within about ±50%. The median T_{max} equals ~2 h with a range from 50 min to 275 min for the CCB cases. Thus the time series analyses suggest time scales of about one to four hours for the lateral mesoscale meanders at CCB.

The CCB data also reveal a dependence of lateral turbulence intensity $i_y = \sigma_v u^{-1}$ on wind speed similar to that exhibited by the data in Fig. 1. Hourly average i_y and u are plotted in Fig. 6, illustrating that i_y is small and well-behaved for high wind speeds but is large and scattered for low wind speeds. These data suggest that hourly average σ_v is equal to ~0.50 m s^{-1} during average nighttime conditions over the Snake River Plain in Idaho. The magnitude of σ_v here is midway between that observed over flat grassland in England and mountainous terrain in California.

The information in Figs. 3 through 5 can be used to develop an empirical formula for average hourly lateral turbulence intensity i_y that is based on hourly wind speed and direction data. We see in Figs. 3 and 5 that there is often much mesoscale energy at time scales greater than the one-hour averaging time for meteorological variables at CCB, but also that there are fluctuations at time scales less than one hour. It is reasonable to break up average hourly i_y into two independent components—a component i_{y1} accounting for eddies with time scales greater than one hour and a component i_{y2} accounting for eddies with time scales less than one hour:

$$i_y^2 = i_{y1}^2 + i_{y2}^2. \quad (4)$$

We assume that the large-scale component i_{y1} is caused entirely by changes in mean wind direction from hour-to-hour:

$$i_{y1} = \tan[0.145(|\Delta WD_-| + |\Delta WD_+|)], \quad (5)$$

if ΔWD_- and ΔWD_+ are the same sign, or

$$i_{y1} = \tan[0.145\ \mathrm{MAX}(|\Delta WD_-|, |\Delta WD_+|)], \quad (6)$$

if ΔWD_- and ΔWD_+ are different sign, where

ΔWD_- = wind direction (degrees) at hour of interest minus wind direction at previous hour
ΔWD_+ = wind direction (degrees) at next hour minus wind direction at hour of interest.

In this equation wind direction is in degrees and it is assumed that the standard deviation of a uniform

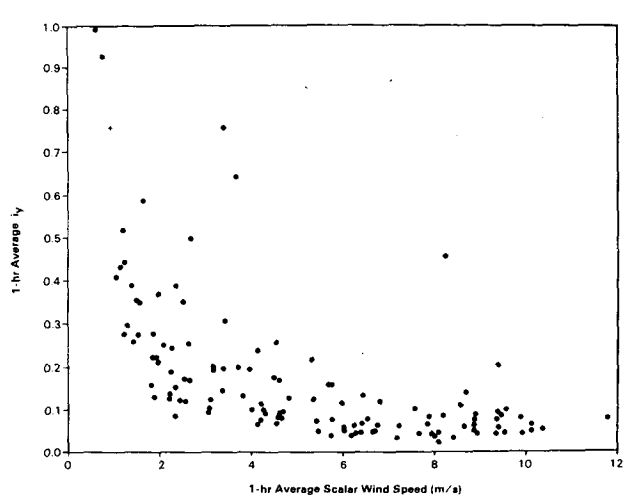

FIG. 6. Average hourly lateral turbulence intensity i_y as a function of wind speed u from Cinder Cone Butte experiment. Most data are from the 40 m tower level; on a few occasions when the 40 m data are not available, the 80 m level is substituted.

distribution equals 0.29 times the width of the distribution. Even if there is no small scale turbulence, a change in wind direction of 40° over a two-hour period centered on the hour of interest will result in an i_y of 0.10.

The small scale component i_{y2} is assumed to be given by the formula:

$$i_{y2} = \sigma_{v2}u^{-1} = (0.5 \text{ m s}^{-1})u^{-1}, \quad (7)$$

where u is the hourly averaged wind speed in m s^{-1} and $\sigma_{v2} = 0.5$ m s^{-1} is a site-specific constant. This formula is consistent with the data in Figs. 1 and 5, implying that σ_{v2} is nearly constant during stable conditions at any site. We have looked at data from several other sites and find that σ_{v2} ranges from about 0.3 to 1.0 m s^{-1}, depending on local effects such as topography, synoptic conditions, and coastal influences. Predictions of average hourly i_y made using Eq. (4) are compared with observations of i_y at the 10 m level of the CCB tower in Fig. 7, showing that the predictions are fairly good on the average, and that 94% of the observations are within a factor of two of the predictions. The underprediction of the highest six observed i_y values is probably caused by our smoothing procedure for hour-to-hour wind direction changes. If all the wind direction change occurred during a short period, the i_{y1} value calculated by Eq. (5) or (6) would be a factor of two low.

4. Observations of lateral dispersion

Lidar observations of the plume upwind of the Butte were used to estimate cross-wind diffusion, as indicated by σ_y, the standard deviation of the lateral concentration distribution. Lidar data were available from less than half the experiments included in Table 1. Nearly instantaneous plume observations σ_{yi} were obtained from individual lidar cross-sections and the total hourly σ_y was estimated by taking the sum of the squares of the instantaneous values and the plume centroid displacements:

$$\sigma_y^2 = \sum_{i=1}^{n} \sigma_{yi}^2 n^{-1} + \sum_{i=1}^{n} (y_{ci} - \bar{y}_c)^2 n^{-1}. \quad (8)$$

The first and last terms can be thought of as σ_{yt}^2 and σ_{yc}^2, or the contribution to total σ_y due to small-scale turbulence and plume centroid position fluctuations, respectively. The parameter y_c is the centroid position, and n is the number of lidar cross-sections at the particular downwind distance during that hour (usually $n \sim 10$). The contribution to σ_y from lateral displacement of centroids or meandering is greater than the individual scan contribution in about 50% of the cases analyzed. In 20% of the cases, the meander component exceeds the individual scan component by a factor of 5–10. High values of σ_y/σ_{yt} are sometimes observed for all wind speeds less than about 6 m s^{-1} and are never observed for wind speeds greater than 6 m s^{-1}.

If we assume that $F_y(x)$ equals unity at small distances in Eq. (2), then observed lidar σ_y's upwind of the hill should approximate $i_y x$, where i_y is obtained for the source height by linear interpolation from adjacent tower levels. In Fig. 8, the hourly averaged σ_y's are plotted versus $i_y x$ for 13 separate experiment hours. Each hourly σ_y is made up of contributions from individual lidar scans and from the lateral displacement of observed plume centroids [as given in Eq. (8)]. Figure 8 shows that the line $\sigma_y = i_y x$ passes through the middle of the data set, but that the data from individual hours can be as much as a factor of 3 different from this line. The curves for individual hours generally have slopes close to unity. Many factors could contribute to the scatter on the figure, including small sample size, unrepresentative tower i_y, lidar resolution and accuracy, and poor wind instrument response during light and variable winds.

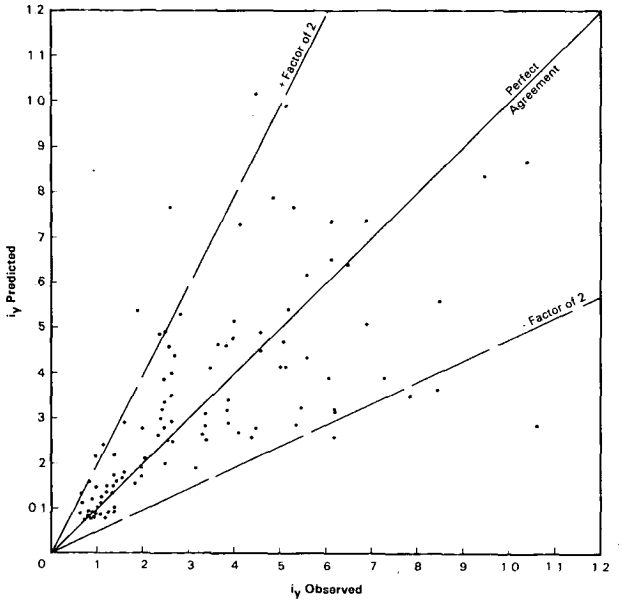

FIG. 7. Observed hourly lateral turbulence intensity at the 10 m level plotted versus predicted hourly lateral turbulent intensity from Eq. (4).

5. Implications of results for diffusion calculations

The presence of mesoscale lateral eddies with periods of about two hours during stable conditions has been confirmed by analysis of 17 overnight experiments at CCB. When averaging times for meteorological and concentration data are one hour, about one-half to one full cycle can be expected to be captured during periods when these mesoscale eddies are present. It is possible that the winds will continually decrease or increase during the 1 h period, or decrease for the first 30 min and increase for the last 30 min of the period, depending on the portion of the sinusoidal wind cycle

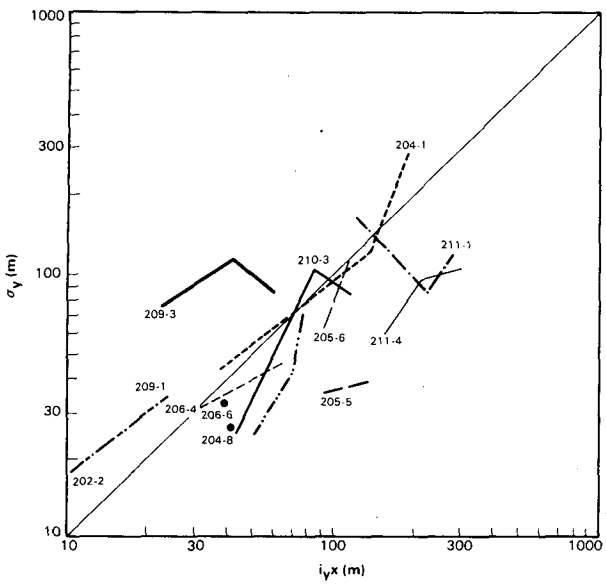

FIG. 8. Observed hourly σ_y plotted as a function of $i_y x$ for selected experiment hours.

that is captured (see Fig. 3). This mesoscale energy thus appears as a trend or a slow meander during a 1-hour period rather than as a turbulent fluctuation. Because these time scales are comparable to the averaging periods of interest, the effects of mesoscale meander must be accounted for explicitly. It is best to use observations of σ_θ, i_y, or the actual hourly probability distributions of wind direction (rather than some conjectured distribution) to model hourly average plume transport and impacts. If the distribution of wind direction is clearly non-Gaussian, then it is important that the actual distribution be used in place of the Gaussian shape in a diffusion model. Kristensen *et al.* (1981) suggest that if the dispersion by meandering is not taken into account, estimates of mean concentrations can easily be a factor of 4–6 too high. If no fluctuation data are available, then an empirical formula [Eq. (4)] can be used to estimate hourly average i_y from hourly records of mean wind speed and direction.

Acknowledgments. This work was performed under Contract Number EPA-600/3-82-036 from the U.S. Environmental Protection Agency. Much of the computer output was generated by Donald DiCristofaro and John Beebe.

REFERENCES

Cooley, J. W., and J. W. Tukey, 1965: An algorithm for the machine calculation of complex Fourier series. *Math. Comput.*, **19,** 297–301.

Deardorff, J. W., 1974: A three-dimensional numerical study of the height and mean structure of a heated planetary boundary layer. *Bound.-Layer Meteor.*, **1,** 81–106.

Gifford, F. A., 1976: Turbulent diffusion typing schemes—A review. *Nucl. Saf.*, **17,** 68–86.

Hanna, S. R., 1981a: Diurnal variation of horizontal wind direction fluctuations σ_θ in complex terrain at Geysers, CA. *Bound.-Layer Meteor.*, **58,** 207–213.

——, 1981b: Lagrangian and Eulerian time-scale relations in the daytime boundary layer. *J. Appl. Meteor.*, **20,** 243–249.

Kristensen, L., N. O. Jensen and E. L. Peterson, 1981: Lateral dispersion of pollutants in a very stable atmosphere—The effect of meandering. *Atmos. Environ.*, **15,** 837–844.

Lavery, T. F., A. Bass, D. G. Strimaitis, A. Venkatram, B. R. Greene, P. J. Drivas and B. A. Egan, 1982: EPA complex terrain model development program. *First Milestone Report*—1981. EPA-600/3-82-036, U.S. EPA, Research Triangle Park, NC, 304 pp.

Lemone, M. A., 1978: The marine boundary layer. *Proc., Workshop on the Planetary Boundary Layer,* Amer. Meteor. Soc., 182–234.

NRC, 1979: *Atmospheric Dispersion Models for Potential Accident Consequence Assessments at Nuclear Power Plants.* Reg. Guide 1.145, U.S. NRC.

Pasquill, F., 1974: *Atmospheric Diffusion,* 2nd ed. Wiley and Sons, 429 pp.

——, 1976: Atmospheric dispersion parameters in Gaussian plume modeling: Part II. Possible requirements for change in the Turner workbook values. Rep. EPA-600/4-760306, U.S. EPA, 44 pp.

Rayment, R., 1970: Introduction to the Fast Fourier Transform (FFT) in the production of spectra. *Meteor. Mag.*, **99,** 261–269.

Sagendorf, J. F., and C. R. Dickson, 1974: *Diffusion Under Low Windspeed, Inversion Conditions.* NOAA Tech. Memo ERL ARL-52, U.S. Dept. Commerce, 89 pp.

Schacher, G. E., C. W. Fairall and P. Zannetti, 1982: Comparison of stability classification methods for parameterizing coastal overwater dispersion. *Proc., First Int. Conf. Meteor. and Air-Sea Interaction of the Coastal Zone,* The Hague, Amer. Meteor. Soc., 91–96.

Smith, F. B., and P. F. Abbott, 1961: Statistics of lateral gustiness at 16 meters above ground. *Quart. J. Roy. Meteor. Soc.*, **87,** 549.

VanderHoven, I., 1976: A survey of field measurements of atmospheric diffusion under low wind speed inversion conditions. *Nucl. Saf.*, **17,** 223–230.